UDC 62-562
DOI: 10.15587/1729-4061.2025.337849

SUBSTANTIATING THE OPTIMAL SHAPE OF A BIMETAL FLYWHEEL

Sergey Ryagin
Corresponding author
PhD, Associate Professor*
E-mail: ryaginzp@gmail.com
Roman Onyshchenko
PhD Student*
Volodymyr Shevchenko
PhD, Associate Professor*
Serhii Shumykin
PhD, Associate Professor*
*Department of Theoretical and Applied Mechanics
National University "Zaporizhzhia Polytechnic"
Zhukovskoho str., 64,
Zaporizhzhia, Ukraine, 69063

This study's object is the flywheel as an energy storage device. The task addressed is to devise a sequential approach to flywheel shape optimization.

The analytical basis of flywheel shape optimization has been reconstructed to reveal the source of contradictory results. It was found that the product of radius and angular velocity of rotation is a constant that depends on material properties for the ring-shaped disk flywheel. It becomes somewhat more complicated for other flywheel shapes. It is the reason for the contradictions in the flywheel shape optimization results reported by researchers.

Comparative calculations for several flywheel shapes have been performed using the finite element method. The results confirmed that bringing material closer to the axis of rotation, including Laval disk shape, does not give any advantages. Material choice has an essential advantage in comparison with shape optimization. The flywheel shape has to be optimized together with the material. A ring-shaped disk flywheel is a good starting point for flywheel shape optimization. The results are attributed to the nature of the flywheel material behavior under the action of inertia forces.

A novel approach to combining different materials in flywheel construction has been proposed. One material (high-strength steel) was used for the flywheel ring. Another material with a lower elastic modulus (high-strength aluminum alloy) was used for elements connecting the ring with the shaft. The bimetal flywheel has a mass three times less than the base variant, with 24.6% underload for steel parts and 17.3% underload for aluminum parts.

The findings reported here could be practically implemented in the design and manufacturing of flywheel energy storage systems with increased specific energy for use in vehicles and stationary power units

Keywords: flywheel shape optimization, specific energy, bimetal structure, finite element method

Received 06.06.2025
Received in revised form 31.07.2025
Accepted 18.08.2025
Published 28.08.2025

How to Cite: *Ryagin, S., Onyshchenko, R., Shevchenko, V., Shumykin, S. (2025). Substantiating the optimal shape of a bimetal flywheel. Eastern-European Journal of Enterprise Technologies, 4 (7 (136)), 23–31. https://doi.org/10.15587/1729-4061.2025.337849*

1. Introduction

The growing demand for energy storage is characteristic of modern mobile and stationary technical means. Therefore, the use of flywheels as devices for energy storage is one of the main directions of development of modern energy systems. Scientific research on this topic is important because only the generation of new technical solutions can ensure the development of this promising environmentally safe area of energy equipment design. The results of such research are necessary for practical application as they contribute to reducing mass, improving dynamic characteristics, reducing cost, and increasing the efficiency of flywheel structures. Thus, research into this area is extremely relevant.

2. Literature review and problem statement

In [1], the results of studies on the search for the optimal shape of the flywheel are reported. An attempt is made to link the specific energy of the flywheel and the strength of its material via a certain shape factor. This factor is used as a measure of the use of flywheel material. Its highest value is given for the Laval disk, slightly lower for a disk with a rectangular cross-section. However, the results acceptable for a linear stress state cannot be properly and correctly extended to flat and volumetric stress states using this artificial factor.

Work [2] also describes the results of a study on the search for the optimal shape of the flywheel. The found shape has a pear-shaped cross-section, with the metal displaced towards the axis of rotation. This shape also resembles the Laval disk, although it differs from it. Therefore, the cited paper does not contain results that are fundamentally different from [1].

Work [3] reports the results of searching for the optimal shape of the flywheel. The optimal shape is considered to be the Laval disk, as well as a similar disk with a Gaussian cross-section. Therefore, the authors of [3] do not give results that are fundamentally different from those in paper [1].

Study [4] describes the results of research on finding the optimal shape of the flywheel. The advantages of aluminum alloy flywheels are shown without analytical justification. The shape factor was not used. As a result of optimization, the triangular cross-section was recognized as the best. These results do not even agree with the results of research on the flywheel with a rim disk, which were reported in [4].

Paper [5] describes the results from a study on finding the optimal shape of the flywheel with a rim disk. It is shown that the optimization of such a flywheel has some features. However, a flywheel with a rim disk is prone to bending deformations and, accordingly, to local increases in stress. In addition, the use of a flywheel with a rim disk causes high air resistance or requires insulation of the flywheel in a vacuum [6]. All this limits the prospects of flywheels with such a structure.

In [7, 8], the results of research on finding the optimal shape of the flywheel taking into account the plane stress state are reported. During optimization, it was found that the best shape is a flywheel with a small thickening near the axis of rotation and a larger thickening outside. In this case, the results by different authors, obtained by similar methods, are similar to each other, but contradict the findings from [1–4]. In addition, in [7, 8], insufficient attention is paid to the flywheel material.

In [9], the results of studies on finding the optimal shape of the flywheel taking into account the plane stress state are described. The technique for obtaining the solution is somewhat different from that used in [7, 8]. Accordingly, the result is different. Based on work [9], the best shape of the flywheel is similar to that obtained in [7, 8], but slightly closer to cylindrical. But it also contradicts the results reported in [1–4].

In [10], the results of research on optimizing the dimensions of a cylindrical flywheel taking into account the material are described. The problem was solved analytically for a plane stress state. However, optimization of the flywheel shape was not taken into account in the work.

In [11], the results of a study on the analysis of the volumetric stress state of several flywheel designs made of different materials using the finite element method (FEM) are reported. However, these structures were compared but not systematized. The cited work does not provide an analytical justification for comparing designs, and no new types of structures are proposed.

Thus, in works [1–5, 7–11] there is no single approach to optimizing the flywheel shape. The best solutions are considered to be a Laval disk [1], a rectangular cross-section [1, 10], a pear-shaped cross-section [2], a Gaussian cross-section [3], a triangular cross-section [4], a small thickening near the axis of rotation, and a larger thickening outside [7–9]. The authors of [1–4] strive to bring the metal closer to the axis of rotation. The authors of [7–9], on the contrary, are inclined to a constructively balanced distance of the metal from the axis of rotation. These results are contradictory and often mutually exclusive, even in the case of the same problem statement. Whereas the rational choice of material is noted, it is considered separately from the optimization of the flywheel shape. This allows us to argue that it is advisable to conduct a study aimed at searching for a general systematic approach to the optimization of the flywheel shape.

3. The aim and objectives of the study

The aim of our research is to devise a consistent approach to optimizing the shape of the flywheel. This could allow for the design of a promising new flywheel structure.

To achieve the goal, the following tasks were set:

– to reconstruct the analytical basis for optimizing the shape of the flywheel;

– to perform comparative calculations for three typical flywheels;

– to consider simultaneous optimization of the shape and material of the flywheel with the design of a bimetallic structure.

4. The study materials and methods

The object of our study is a flywheel. The principal hypothesis of the study assumes that the inconsistency in the results of optimizing the flywheel shape is due to the fundamental properties of its structure.

The study used both analytical methods that make it possible to identify fundamental relationships between the flywheel parameters as well as FEM, which provides the ability to calculate the volumetric stress state of bodies of complex shape. The properties of materials were taken into account according to the relevant standards for them. It was assumed that the flywheel operates within the proportionality limit of its material. As a simplification, the study assumed that the flywheel moves with a constant angular velocity. Operating modes with angular accelerations were not considered, because they are not fundamental. In addition, it was assumed that the force of gravity can be neglected as relatively small. It was also believed that the issues associated with the flywheel supports go beyond the scope of our study.

5. Results of devising a sequential approach to optimizing the shape of the flywheel

5. 1. Reconstruction of the analytical basis for optimizing the shape of the flywheel

It is well known from theoretical mechanics that it is the annular shape of the flywheel (Fig. 1) that provides the greatest value of the ratio of its kinetic energy T to mass M (specific energy W). For such a shape, the moment of inertia I

$$I = M \cdot R^2, \tag{1}$$

where R is the radius of the ring.

Accordingly, kinetic energy has been defined as

$$T = 0.5 \cdot I \cdot \omega^2 = 0.5 \cdot M \cdot R^2 \cdot \omega^2, \tag{2}$$

where ω is the angular speed of rotation of the flywheel, rad/s.

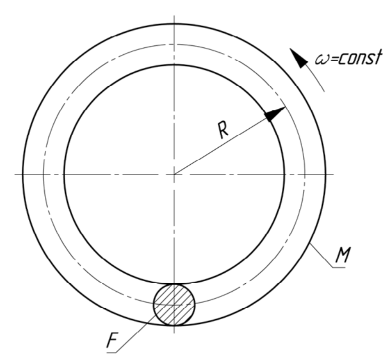

Fig. 1. Ring-shaped flywheel

The specific energy was calculated as

$$W = \frac{T}{M} = 0.5 \cdot R^2 \cdot \omega^2. \tag{3}$$

The relationship with the strength parameters was determined from the calculation scheme shown in Fig. 2. When rotating at a constant angular velocity, an infinitely small segment of the flywheel with an angular size $d\alpha$ is acted upon by a uniformly distributed centrifugal force q, which is balanced by longitudinal internal forces N. In the projection onto the vertical axis, the equilibrium equation takes the form

$$2 \cdot N \cdot \sin\frac{d\alpha}{2} = q \cdot R \cdot d\alpha. \quad (4)$$

Equation (4) has been simplified given that the sine of an infinitesimal angle is approximately equal to the angle itself

$$N = q \cdot R. \quad (5)$$

Distributed centrifugal force q

$$q = \frac{dm \cdot \omega^2 \cdot R}{R \cdot d\alpha}, \quad (6)$$

where dm is the mass of the smallest sector of the flywheel

$$dm = \rho \cdot F \cdot R \cdot d\alpha, \quad (7)$$

where ρ is the density of the flywheel material, kg/m^3; F is the cross-sectional area of the ring, m^2.

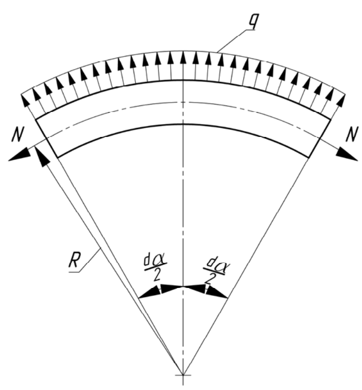

Fig. 2. Calculation diagram

Substituting (7) in (6), we obtained

$$q = \rho \cdot F \cdot \omega^2 \cdot R. \quad (8)$$

Substituting (8) into (5), we obtained

$$N = \rho \cdot F \cdot \omega^2 \cdot R^2. \quad (9)$$

Accordingly, normal stresses σ, Pa

$$\sigma = \frac{N}{F} = \rho \cdot \omega^2 \cdot R^2. \quad (10)$$

The result (10) fully corresponds to the result obtained by another method in [12], which confirms its correctness.

In a rational structure of a flywheel, it is necessary to strive for equal strength. Since the material of the ring must be maximally loaded, in the condition of strength the inequality was replaced by equality

$$\sigma = \rho \cdot \omega^2 \cdot R^2 = [\sigma], \quad (11)$$

where $[\sigma]$ is the permissible stress, Pa.

Then

$$\omega^2 \cdot R^2 = \frac{[\sigma]}{\rho}. \quad (12)$$

Substituting (12) in (3), we obtained

$$W = 0.5 \cdot \frac{[\sigma]}{\rho}. \quad (13)$$

The result (13) in one form or another is noted in various literary sources and serves as the basis for the conclusion about the rationality of using those materials in flywheels that simultaneously have low density and high strength characteristics. As a rule, titanium and aluminum alloys are termed as such materials, as well as more modern and expensive materials. High-strength aluminum alloys could be a rational choice taking into account the factor of economic feasibility.

However, when searching for a rational shape of the flywheel cross-section, it should be taken into account that formula (12) can be rewritten in the form

$$\omega \cdot R = \sqrt{\frac{[\sigma]}{\rho}}. \quad (14)$$

From formula (14) it is clear that when the material is selected, the minimum mass of the flywheel is already predetermined. The designer may prefer to increase the angular velocity or, conversely, increase the radius, taking into account the specific requirements for dimensions, supports, and drive, but this will not have a significant impact on the mass.

From the point of view of shape optimization, there is a contradiction: moving the material away from the axis of rotation increases the moment of inertia, but moving the material closer to the axis of rotation reduces stress and allows for an increase in the rotational speed. The situation is somewhat complicated if we consider that the flywheel ring must be somehow connected to the shaft, and the cross-section of this ring has specific dimensions and shape. Accordingly, radial stresses are added to the circumferential ones, which corresponds to a plane stress state. In fact, a volumetric stress state emerges.

In essence, formula (14) means that any objective function related to the rational use of flywheel material will take a very complex form with a large number of local extrema. This is why the results of flywheel shape optimization obtained by different researchers are so different from each other.

5. 2. Performing comparative calculations for three typical flywheels

To illustrate the above, a comparative calculation was performed for two specific flywheels that have common features and differences. A sketch of a flywheel made of ordinary steel in the form of a cylinder, the metal of which is relatively close to the axis of rotation, is shown in Fig. 3. A sketch of a flywheel made of high-strength aluminum alloy in the form of a disk with the metal mainly remote from the axis of rotation, is shown in Fig. 4. Both flywheels are mounted on a shaft with the same diameter of 80 mm, have the same rotational speeds and moments of inertia (Table 1). The results from determining the stress state using FEM for both flywheels are shown in Fig. 5, 6, respectively, and are also summarized in Table 1.

From the analysis of Fig. 5 it is obvious that the stresses are distributed over the flywheel extremely unevenly.

The maximum stresses act in the area of attachment of the flywheel to the shaft. From the analysis of Fig. 6 it is obvious that the maximum stresses act in the elements connecting the outer ring to the shaft. These are mainly radial stresses.

From the analysis of Table 1 it is obvious that the steel flywheel has a smaller radial size but loses in width. However, the flywheel made of high-strength aluminum alloy is 4.6 times lighter than the steel one, despite the fact that they have approximately the same kinetic energy, and the steel flywheel is overloaded by 3.3% while the aluminum one is underloaded by 11.4%. Accordingly, the specific energy of the aluminum flywheel is also 4.6 times higher than that of the steel one. This is due, first of all, to the advantage of the material, although the shape also has a certain secondary importance.

To check the influence of the flywheel shape, another calculation was carried out. For this purpose, a flywheel in the form of a Laval disk was used. This Laval disk was made of the same material: high-strength aluminum alloy, which was used in the second version. A sketch of the third flywheel is shown in Fig. 7. Its dimensions were chosen so that they were comparable with the second flywheel and the flywheel in the form of a Laval disk would have approximately the same moment of inertia as the first and second variants. From Fig. 7 it is obvious that this flywheel also has a tendency to shift the material towards the axis of rotation, although from the point of view of logic the concave shape of the curves would be more suitable for the given purpose than the convex one. The use of the Laval disk shape expectedly allowed us to increase the rotation speed to 7250 min^{-1}, which is 1.17 times more than in the first two variants. Accordingly, the square of the speed will be 1.37 times greater. The results from determining the stress state of the third flywheel are shown in Fig. 8 and are summarized in Table 1.

From the analysis of Table 1, it is clear that the flywheel in the form of a Laval disk is only 1% underloaded, but its mass is 1.75 times greater than that of the second variant. Although the kinetic energy also increased by approximately the same 1.37 times due to the increase in rotation speed, the specific energy turned out to be 1.28 times lower than that of the second flywheel due to the increase in mass.

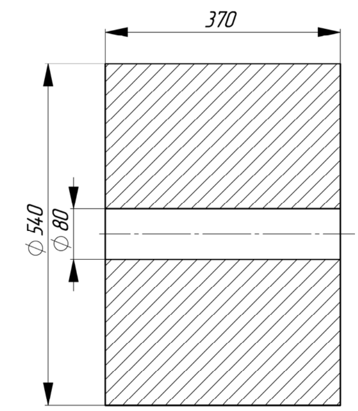

Fig. 3. Sketch of a cylindrical flywheel

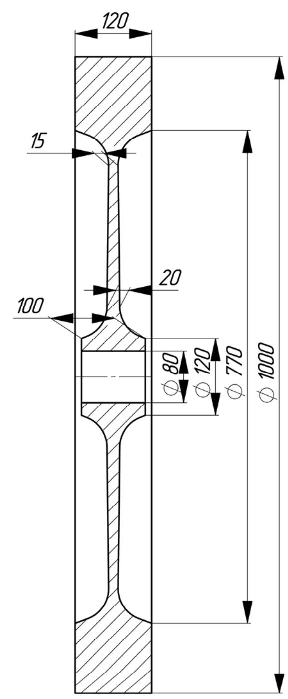

Fig. 4. Sketch of a ring-shaped flywheel

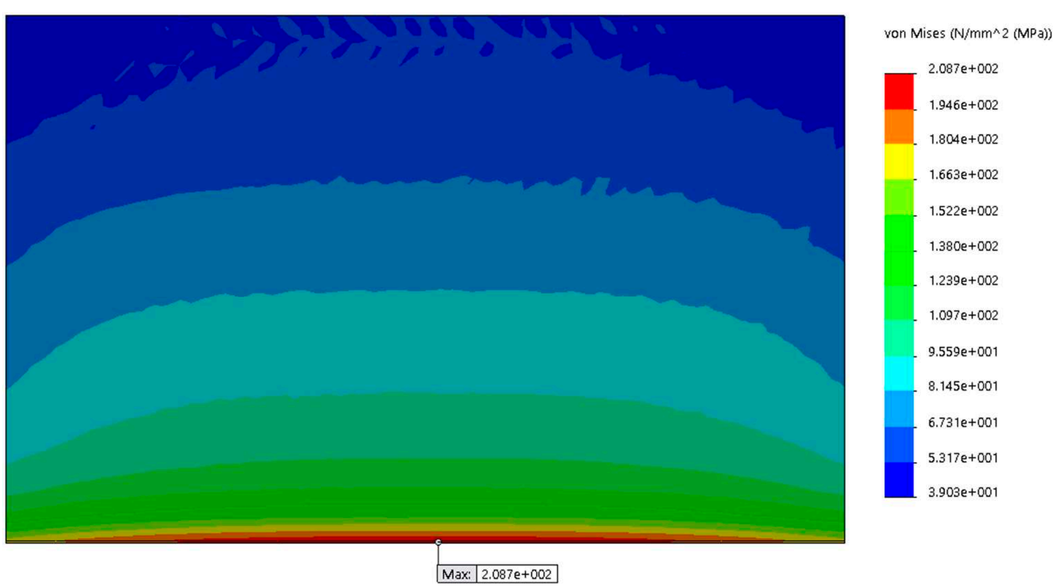

Fig. 5. Stress state of a cylindrical flywheel

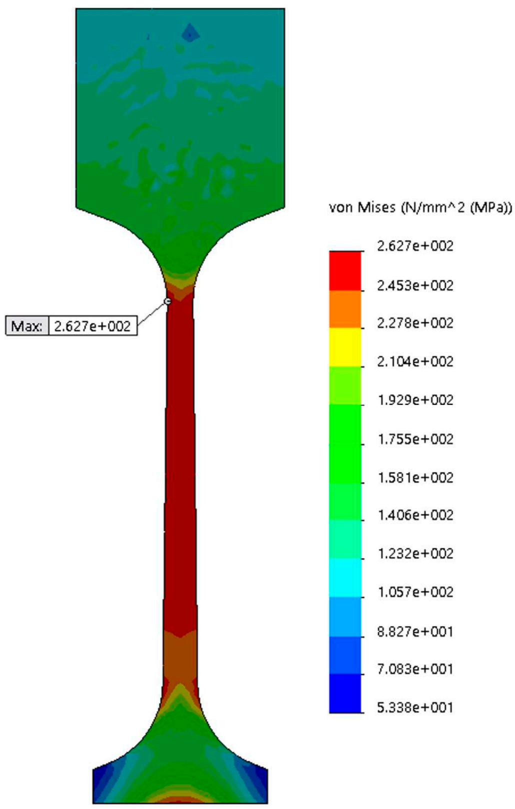

Fig. 6. Stress state of the ring-shaped flywheel

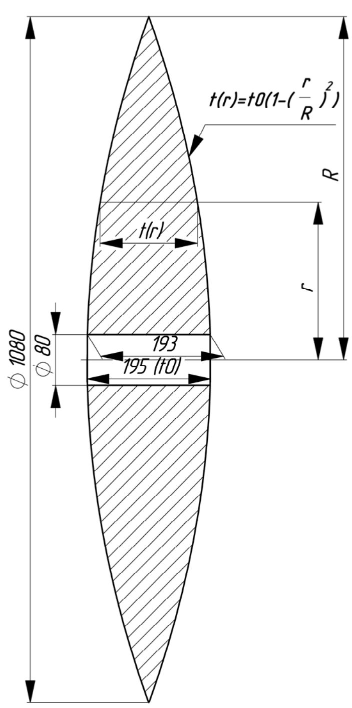

Fig. 7. Sketch of a flywheel in the shape of a Laval disk

Thus, the fashionable form of the Laval disk turned out to be significantly worse than the traditional annular form, even with a smaller underload. Moreover, the displacement of the material closer to the axis of rotation does not give any advantages. On the other hand, the choice of material has a significant advantage compared to the optimization of the shape.

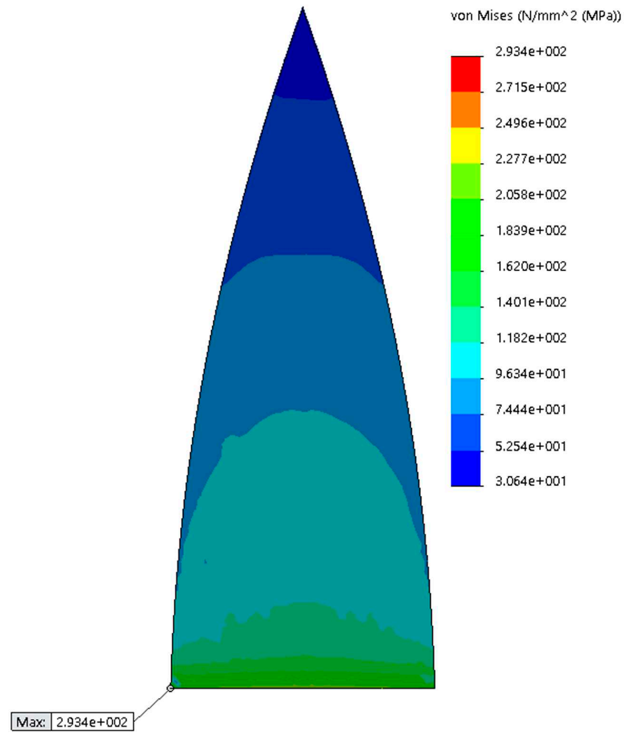

Fig. 8. Stress state of the flywheel in the shape of a Laval disk

Table 1

Results

Variant	1	2	3	4
Shape	Cylindrical	Annular	Laval disk	Ring-shaped
Figures	3, 5	4, 6	7, 8	9, 10
Material	Carbon steel 1023 (ASTM)	High-strength aluminum alloy 2014-T6 (ASTM)	High-strength aluminum alloy 2014-T6 (ASTM)	Bimetal (High-strength steel 30KhGSA DSTU 7806:2015 / High-strength aluminum alloy 2014-T6)
Density, kg/m^3	7,858	2,800	2,800	7,850 / 2,800
Modulus of elasticity, GPa	205	72.4	72.4	215 / 72.4
Yield strength, MPa	282.7	415	415	830 / 415
Permissible stresses, MPa	202	296.4	296.4	592.8 / 296.4
Maximum calculated stress, MPa	208.7	262.7	293.4	447.0 / 245.2
Maximum diameter, mm	540	1000	1080	750
Maximum width, mm	370	120	193	168
Mass, kg	651	141.3	246.7	215 (210 / 5)
Moment of inertia, kg·m^2	24.26	24.27	24.2	24.4
Angular velocity, min^{-1} (rad/s)	6,200 (649.26)	6,200 (649.26)	7,250 (759.22)	6,200 (649.26)
Kinetic energy, MJ	5.113	5.115	6.975	5.143
Specific energy, J/kg	7,854.5	36,202.2	28,271.7	23,919.9

5. 3. Simultaneous optimization of the flywheel shape and material with the design of a bimetallic structure

It is obvious that another way is needed to improve the flywheel shape. Such a way became clear from the analysis of Fig. 6. It is necessary to reduce the radial stresses in the elements connecting the ring to the shaft by increasing the circumferential stresses in the ring. This is possible when using one material for the ring and another material with a lower modulus of elasticity for the elements connecting it to the shaft.

In general, this is, in fact, a way to resolve the above contradiction. The flywheel shape should be optimized together with the material. According to our results, the annular flywheel is the correct starting point for optimizing the flywheel shape. Moreover, in the case of a bimetallic flywheel, no numerical procedure is even needed since the starting point will simultaneously be the end point due to design constraints.

Strategically, the use of a rim-disc flywheel is an attempt to implement the same trend but with limited means. However, the production of composite flywheels [13] is significantly different from this trend and refers to a different problem [14, 15] related to flywheels.

The use of multi-disk (multi-layer) structures [16, 17] has a similar goal of redistributing mainly radial stresses. However, different results are achieved: radial stresses are redistributed mainly not into circumferential stresses, but into radial loads in the connections between the disks (layers). On the other hand, the simultaneous use of different materials provides new opportunities in the design of flywheels.

A slightly closer technical solution is to use materials with lower strength in areas with insignificant stresses or to use anisotropic materials taking into account the direction of stress action [18]. But such a complex and expensive approach does not solve the problem of stress redistribution.

The closest technical solution is to manufacture a flywheel by winding thin threads of different strong and flexible materials onto the hub. This idea was patented, developed, and described in detail in [19]. However, this technical solution is associated not only with the problem of fixing the ends of the wound material but also with various vibration effects, inevitable even with perfect initial balancing. Thus, the body on which the winding is carried out remains a separate flywheel made of a monomaterial. An attempt to bind the threads in the form of an anisotropic composite material [20] leads to a new problem: such a material does not resist radial loads well. And even the transformation of this composite ring into a multi-disk structure by analogy with [16] does not provide the necessary redistribution of radial and circumferential stresses.

The proposed solution involves an inextricable connection of the ring with other elements, despite the fact that they are made of different materials. The structure, the sketch of which is shown in Fig. 9, was considered as a deliberately imperfect example. The ring is made of high-strength steel 30KhGSA DSTU 7806:2015 [21], other elements are made of the same high-strength aluminum alloy that was used in the two previous versions of the flywheel. The moment of inertia and the speed of rotation of this flywheel correspond to the first and second versions. The basic dimensions of the flywheel, determined taking into account (14), are shown in Fig. 9 and in Table 1. The structure was designed as underloaded (preliminary design stress 465 MPa), for a first approximation, taking into account the need to connect dissimilar materials.

Estimation of the relative circumferential deformation ε_{ts} during deformation of a free steel ring by inertia forces, taking into account (10) and data from Table 1

$$\varepsilon_{ts} = \frac{\sigma_{ds}}{E_s} = \frac{465 \cdot 10^6}{2.15 \cdot 10^{11}} = 2.16 \cdot 10^{-3}, \quad (15)$$

where E_s is the modulus of elasticity of steel; σ_{ds} is the preliminary design stress for the steel ring.

The relative radial strain ε_{rs} will obviously be equal to the relative circumferential strain ε_{ts} since the perimeter of the ring is proportional to its radius. A zero-thickness disk made of high-strength aluminum alloy was added between the steel ring and the shaft. The relative circumferential and radial strains are approximately equal to ε_{rs} and ε_{ts} at the point of its connection with the ring. Taking into account the value of the modulus of elasticity for the high-strength aluminum alloy E_a from Table 1, the circumferential σ_{ta} and radial σ_{ra} stresses were equal to

$$\sigma_{ta} = \sigma_{ra} = E_a \cdot \varepsilon_{ts} = 156.4 \text{ MPa}. \quad (16)$$

Equivalent Mises stress $\boldsymbol{\sigma}_m$ in a zero-thickness disk made of high-strength aluminum alloy for a plane stress state

$$\sigma_m = \sqrt{\frac{1}{2} \cdot \left[\sigma_{ta}^2 + \sigma_{ra}^2 + \left(\sigma_{ta} - \sigma_{ra} \right)^2 \right]}. \quad (17)$$

According to (17), $\sigma_m = 156.4$ MPa as well. These stresses will be higher at non-zero thickness of the disk, closer to the axis of rotation and during acceleration of the flywheel. However, there is almost a double margin before reaching the allowable stress of 296.4 MPa, which ensures the realism of the proposed technical solution.

These analytical calculations were also checked using FEM. The results from determining the stress state of the fourth flywheel are shown in Fig. 10 and are also summarized in Table 1. From the analysis of Table 1 it is obvious that the analytical assumptions, taking into account the non-zero thickness of the disk made of high-strength aluminum alloy, are generally confirmed.

The flywheel is underloaded by 24.6% for steel and by 17.3% for aluminum alloy. However, its mass is three times less than that of the first variant. And although it is larger than that of the second variant, it is smaller than that of the third. At the same time, there is an advantage in overall dimensions compared to both of these variants.

In terms of specific energy, there is an advantage compared to the first variant by 3.05 times. The specific energy is predictably somewhat lower, but comparable to the second and third variants made of high-strength aluminum alloy. However, if the fourth variant is additionally loaded by increasing the rotation speed by 8%, its specific energy will be equal to the specific energy of the third variant.

It is quite reasonable to assume that if in the proposed technical solution, the ring is made of a high-strength aluminum alloy, and the disk is made of a material with an even lower modulus of elasticity and density, then the value of the specific energy will be much higher than in all the options considered here.

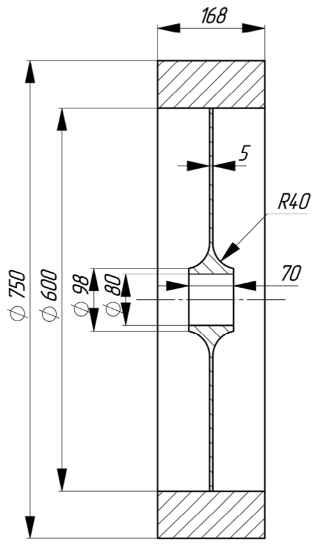

Fig. 9. Sketch of a ring-shaped bimetallic flywheel

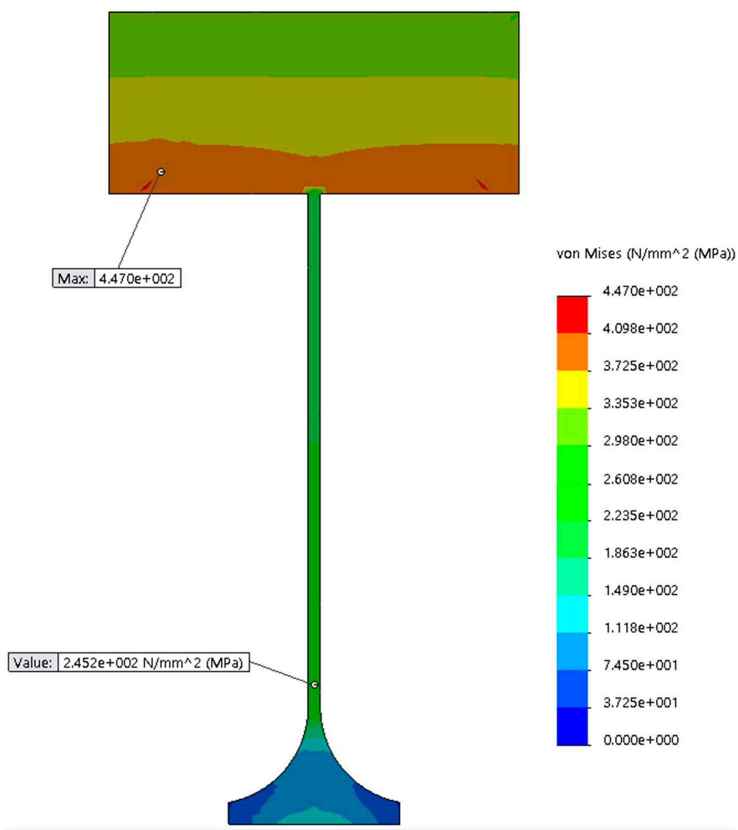

Fig. 10. Stress state of a ring-shaped bimetallic flywheel

6. Discussion of results related to devising a sequential approach to optimizing the shape of the flywheel

Our results are reflected at the analytical level for the linear stress state in formula (14), which shows the most fundamental relationships between the main parameters of the flywheel. For the volumetric stress state, the results obtained are more clearly displayed in Fig. 5, 6, 8, 10, and in Table 1. In particular, Fig. 5, 6, 8 show the distribution of stresses in flywheels of different designs. Figure 10 illustrates the redistribution of stresses in the proposed bimetallic design. These results can be attributed to the very nature of the processes that occur in the flywheel material under inertial loads.

Unlike works [1–5, 7–11], which only consider the optimization of the shape and dimensions of a flywheel made of a predetermined material, the optimization of the flywheel shape together with the material allowed us to avoid contradictory results and to propose an excellent approach to the design. The advantages are provided primarily due to this feature of the proposed solutions. It is from the optimization of the flywheel shape together with the material that the decision to use one material for the flywheel ring and another material with a lower elastic modulus for the elements connecting it to the shaft follows. It was also shown that the annular flywheel is the correct starting point for shape optimization. In particular, the authors of [1–4] reported results that bring the metal closer to the axis of rotation. The authors of [7–9] described results that, on the contrary, move the metal away from the axis of rotation. In our study, solutions are proposed that redistribute stresses within the bimetallic structure. These solutions are the basis of a general systematic approach to optimizing the flywheel shape. They completely avoid the inconsistency of results found by other researchers because optimizing the flywheel shape together with the material changes the very nature of the objective function. In addition, design constraints further eliminate the possibility of obtaining contradictory solutions.

One of the sources that confirm the results is the data from literature. In particular, work [5] reports data on a steel flywheel with a rim disk. This provides an opportunity to compare with the first and fourth calculation options, where the main material is also steel, and the shape and dimensions are also comparable. Thus, for the flywheel in Fig. 3 (the first, basic option) according to Table 1, the specific energy is 7854.5 J/kg. According to [5], the specific energy is 10493 J/kg. Such an increase is natural because the shape of the flywheel with a rim disk is more perfect than that of the cylindrical one. For the bimetallic flywheel in Fig. 9 (the fourth option) according to Table 1, the specific energy is 23919.9 J/kg. Such an increase is also natural because the design and combination of materials of the bimetallic flywheel are even more perfect.

The practical significance of our work is the possibility of improving the design of the flywheel. In particular, reducing the mass of the flywheel while maintaining its energy capacity and using traditional materials leads to a decrease in the mass and cost of other parts and devices that work in a single complex with the flywheel. This contributes to improving dynamic characteristics, reducing costs, and simplifying installation and maintenance. The overall result is an increase in the efficiency of the device. This is especially important for mobile vehicles where flywheels are increasingly used as energy storage devices.

The limitations of our results that must be taken into account when applying them are the failure to take into account the influence of non-stationary operating modes, as well as the failure to take into account the force of gravity and the vibration processes that it causes during rotation.

The disadvantage of the current study is that only one pair of bimetallic flywheel materials was considered. Another disadvantage is the lack of experimental verification, which is beyond the scope of our study. However, the design results taking into account analytical formulas (14) and (17), shown in the form of sketches in Fig. 3, 4, 9, led to an acceptable correspondence between the maximum design stresses obtained using FEM (Fig. 5, 6, 10) and the allowable stresses (data are summarized in Table 1). Therefore, it can be stated that the results of calculations obtained by different methods also indirectly confirm each other.

To build on our study, it is planned to conduct a comparative calculation of a flywheel with a ring made of high-strength aluminum alloy and a disk made of alternative materials. Such a choice of materials is due to the expected significant increase in specific energy, which opens up prospects for reducing mass, improving dynamic characteristics, reducing cost, and overall increasing the efficiency of the structure. After obtaining theoretical results, experimental studies are planned to confirm them.

7. Conclusions

1. For a ring-shaped flywheel, the limiting product of the radius and the angular velocity of rotation is determined by the characteristics of the material and remains a constant value. For flywheels of other shapes, this dependence becomes more complicated, which is one of the reasons for the contradictory optimization results reported in scientific literature. The use of the so-called shape coefficient, which should characterize the efficiency of material use depending on the geometry, does not eliminate the specified problem and in some cases even exacerbates it.

2. Bringing the material closer to the axis of rotation, including the use of a Laval disk, does not provide any advantages. Analysis reveals that the choice of material has a much greater impact on the efficiency of the flywheel than the optimization of its shape.

3. It is proposed to optimize the shape of the flywheel simultaneously with the material. This approach eliminates the contradiction of optimization results due to the change in the nature of the objective function. It is advisable to use a ring-shaped flywheel as an initial configuration for further optimization. In the case of a bimetallic structure, this initial configuration is simultaneously final due to the existing design restrictions. A promising technical solution is to use one material with a high modulus of elasticity for the flywheel ring and another material with a lower modulus of elasticity for the elements connecting the ring to the shaft. In particular, a bimetallic flywheel of annular shape has a specific energy 3.05 times higher compared to the basic version.

Conflicts of interest

The authors declare that they have no conflicts of interest in relation to the current study, including financial, personal, authorship, or any other, that could affect the study, as well as the results reported in this paper.

Funding

The study was conducted without financial support.

Data availability

All data are available, either in numerical or graphical form, in the main text of the manuscript.

Use of artificial intelligence

The authors confirm that they did not use artificial intelligence technologies when creating the current work.

References

1. Amiryar, M., Pullen, K. (2017). A Review of Flywheel Energy Storage System Technologies and Their Applications. Applied Sciences, 7 (3), 286. https://doi.org/10.3390/app7030286
2. Kale, V., Thomas, M., Secanell, M. (2021). On determining the optimal shape, speed, and size of metal flywheel rotors with maximum kinetic energy. Structural and Multidisciplinary Optimization, 64 (3), 1481–1499. https://doi.org/10.1007/s00158-021-02935-x
3. Coppede, D., da Silva Bortoli, F., Moreira, J. M. L., Magalhaes, N. S., Frajuca, C. (2024). Optimization of Flywheel Rotor Energy and Stability Using Finite Element Modelling. Energies, 17 (12), 3042. https://doi.org/10.3390/en17123042
4. Surwade, P. B. (2017). Design, analysis and optimization of flywheel. Spvryan's International Journal of Engineering Sciences & Technology (SEST), 3 (4), 1–9. Available at: https://www.spvryan.org/archive/Issue3Volume4/18.pdf
5. Jiang, L., Wu, C. W. (2016). Topology optimization of energy storage flywheel. Structural and Multidisciplinary Optimization, 55 (5), 1917–1925. https://doi.org/10.1007/s00158-016-1576-1
6. Rufer, A. (2017). Energy Storage. CRC Press. https://doi.org/10.1201/b22265
7. Singh, P., Chaudhary, H. (2018). Optimal design of the flywheel using nature inspired optimization algorithms. Open Agriculture, 3 (1), 490–499. https://doi.org/10.1515/opag-2018-0054
8. Bhosale, P., Zawar, U. (2022). Shape optimization of flywheel used in agricultural thresher. arXiv. http://dx.doi.org/10.48550/arXiv.2209.02392
9. Kress, G. R. (2000). Shape optimization of a flywheel. Structural and Multidisciplinary Optimization, 19 (1), 74–81. https://doi.org/10.1007/s001580050087
10. Różewicz, M. (2014). Shape optimization of a flywheel. Automatyka/Automatics, 18 (1), 23. https://doi.org/10.7494/automat.2014.18.1.23

11. Jaison, A. A. I., Karuppasamy, K. (2015). Design and optimization of flywheel for automobile applications. International Journal of Mechanical Engineering and Research, 5 (1), 7–13. Available at: https://www.ripublication.com/ijmer_spl/ijmaerv5n1spl_02.pdf
12. Pysarenko, H. S., Kvitka, O. L., Umanskyi, E. S. (1993). Opir materialiv. Kyiv: Vyshcha shkola, 655.
13. Li, X., Mittelstedt, C., Binder, A. (2022). Ein Überblick über kritische Aspekte bei der Konstruktion von Leichtbau-Schwungradrotoren mit Verbundwerkstoffen. E & i Elektrotechnik Und Informationstechnik, 139 (2), 204–221. https://doi.org/10.1007/s00502-022-01005-4
14. Dems, K., Turant, J. (2009). Two approaches to the optimal design of composite flywheels. Engineering Optimization, 41 (4), 351–363. https://doi.org/10.1080/03052150802506521
15. Tzeng, J., Emerson, R., Moy, P. (2006). Composite flywheels for energy storage. Composites Science and Technology, 66 (14), 2520–2527. https://doi.org/10.1016/j.compscitech.2006.01.025
16. Arnold, S. M., Saleeb, A. F., Al-Zoubi, N. R. (2001). Deformation and life analysis of composite flywheel disk and multi-disk systems (NASA/TM-2001-210578). Glenn Research Center. Available at: https://ntrs.nasa.gov/api/citations/20010047395/downloads/20010047395.pdf
17. Yangoz, C., Erhan, K. (2025). High-Speed Kinetic Energy Storage System Development and ANSYS Analysis of Hybrid Multi-Layered Rotor Structure. Applied Sciences, 15 (10), 5759. https://doi.org/10.3390/app15105759
18. Chen, H. L., Zhu, C. S., Ye, P. (2014). A Comparison of Analysis Flywheel Stress Distributions Based on Different Material. Applied Mechanics and Materials, 536-537, 1291–1294. https://doi.org/10.4028/www.scientific.net/amm.536-537.1291
19. Gulia, N. V. (2005). Superflywheels of supercarbon. The Inventor-Rationalizer, 12 (672). Available at: http://www.t-library.net/read.php?mode=image&id=6638&file=6760&page=15
20. Wang, P., Gu, T., Sun, B., Liu, R., Zhang, T., Yang, J. (2022). Design and Performance Analysis of Super Highspeed Flywheel Rotor for Electric Vehicle. World Electric Vehicle Journal, 13 (8), 147. https://doi.org/10.3390/wevj13080147
21. Steel and alloy guide. Available at: https://www.splav-kharkov.com/mat_start.php?name_id=170